USCAP

www.nature.com/labinvest

ARTICLE

Check for updates

Quantitative assessment of Siglec-15 expression in lung, breast, head, and neck squamous cell carcinoma and bladder cancer

Saba Shafi[1], Thazin Nwe Aung[1], Vasiliki Xirou[1], Niki Gavrielatou[1], Ioannis A. Vathiotis[2], Aileen Fernandez[1], Myrto Moutafi[1], Vesal Yaghoobi[1], Roy S. Herbst[3], Linda N. Liu[4], Sol Langermann[4] and David L. Rimm[1]✉

Immune checkpoint blockade with programmed cell death (PD-1)/programmed death-ligand 1 (PD-L1) inhibitors has resulted in significant progress in the treatment of various cancer types. However, not all patients respond to PD-1/PD-L1 blockade, underscoring the importance of identifying new potential targets for immunotherapy. One promising target is the immune system modulator Siglec-15. In this study, we assess Siglec-15 expression in solid tumors, with a focus on lung, breast, head and neck squamous and bladder cancers. Using quantitative immunofluorescence (QIF) with a previously validated antibody, we found increased Siglec-15 expression in both tumor and immune cells in all the four cancer types. Siglec-15 was seen to be predominantly expressed by the stromal immune cells (83% in lung, 70.1% in breast, 95.2% in head and neck squamous cell and 89% in bladder cancers). Considerable intra-tumoral heterogeneity was noted across cancer types. As previously described for non-small cell lung cancer (NSCLC), Siglec-15 expression was seen to be mutually exclusive to PD-L1 in all the four cancer types, although this differential expression was maintained but somewhat diminished in head and neck squamous cell carcinoma (HNSCC). Siglec-15 was not prognostic either for overall survival (OS) or progression-free survival (PFS). In summary, we show broad expression of this potential immune modulatory target in a wide range of cancer types. These data suggest potential future clinical trials in these tumor types.

Laboratory Investigation (2022) 102:1143–1149; https://doi.org/10.1038/s41374-022-00796-6

INTRODUCTION

Immune checkpoint inhibition has revolutionized therapeutic approaches for the treatment of advanced solid cancers and has become the new standard-of-care for advanced cancer patients after progression on conventional therapy, or in some cases, instead of conventional therapy. However, targeting programmed cell death 1 (PD-1)/programmed death-ligand (PD-L1) benefits only about 30% of the non-small cell lung cancer (NSCLC) patients[1,2], around 5% of triple negative breast cancers (TNBC)[3–9], ~13–18% of head and neck squamous cell carcinoma (HNSCC)[10–15] and ~15–29% of urothelial cancers[16–20]. The limited response with PD-1/PD-L1 therapy has underscored the importance of identifying new potential immunotherapeutic targets.

Siglec-15 is a member of the sialic-acid binding immunoglobulin type lectins, a membrane protein, that is normally expressed by cells of the myeloid lineage. Structurally, it consists of a V-set immunoglobulin (Ig) domain containing the sialic acid-binding site and an extracellular region with one or more C2-set Ig domains[21–23]. Importantly, Siglec-15 exhibits high structural homology with B7 family proteins, notably with PD-L1. Unlike other members of the Siglec family, Siglec-15 lacks the immune receptor tyrosine-based inhibition motifs (ITIMs) in its cytoplasmic domain. Instead, it exerts its downstream effects through interactions with signaling adaptor DNAX-activating protein of 12 kDa (DAP12) and DAP10 that contain an immunoreceptor tyrosine-based activation motif (ITAM)[23]. A recent study conducted by Wang et al. highlighted the role of Siglec-15 as a critical immune suppressor as well as emphasized its upregulation across various cancer types. Siglec-15 was shown to be induced by macrophage colony-stimulating factor while interferon-gamma (IFN-γ) released from tumor-infiltrating T-lymphocytes downregulated it. Interestingly, IFN-γ has the opposite effect on PD-L1 expression in tumor micro-environment (TME), causing its upregulation. These unique molecular features and a possible link with PD-L1 highlight the crucial role of Siglec-15 in immune evasion in various cancers, through mechanisms that seem to be independent of PD-1/PD-L1 pathway.

Hence, blockade of Siglec-15 may provide a solution for the emerging need for new strategies for patients resistant to PD-1/PD-L1 inhibition[24]. Currently, a phase II clinical trial is ongoing to test the effectiveness of a monoclonal antibody against Siglec-15 in NSCLC (NC318). Here, we used quantitative immunofluorescence (QIF) to evaluate the patterns of expression and distribution of Siglec-15 across four cancer types including lung, breast, head and neck squamous cell, and bladder cancers. We also assess its correlation with different clinicopathologic characteristics, PD-L1 expression and outcome.

MATERIALS AND METHODS

Patient cohorts, tissue procurements, and TMA construction

We used retrospective serial collections of formalin fixed paraffin embedded specimens from Yale University. A multi-tumor tissue

[1]Department of Pathology, Yale University School of Medicine, New Haven, CT, USA. [2]Department of Medicine, School of Medicine, National and Kapodistrian University of Athens, Athens, Greece. [3]Department of Medicine, Yale University School of Medicine, New Haven, CT, USA. [4]NextCure Inc, Beltsville, MD, USA. ✉email: david.rimm@yale.edu

Received: 17 February 2022 Revised: 19 April 2022 Accepted: 20 April 2022
Published online: 17 May 2022

microarray (YTMA 395) with 210 patient samples from 13 different tumor types was assessed to determine the frequency of Siglec-15 protein expression in a range of tumor types. Retrospective cohorts for lung, breast, bladder and HNSCC were collected and prepared for assessment as tissue microarrays. Table 1 shows the brief overview of the various cohorts used in our study. Details of the baseline characteristics of each cohort can be found in the Supplementary (T1 to T10).

Quantitative immunofluorescence protocol for Siglec-15 and PD-L1

Slides were heated in an oven at 60 °C, de-paraffinized in xylenes twice (20 min each time), then rehydrated with graded ethanol (100% 1 min; 100% 1 min, 70% 1 min) and washed in tap water for 5 min. Antigen was retrieved using ethylene-diamine-tetra-acetic acid (EDTA-0.74 mg in 2 liters of dist. water, pH = 8) at 97 °C for 20 min in a Lab Vision PT Module (Thermo Scientific, Waltham, MA, USA). Endogenous peroxidases were blocked with 2.5% hydrogen peroxide in methanol for 30 min, followed by additional 30 min of incubation with 0.3% bovine serum albumin with 0.05% Tween-20 blocking solution. For Siglec-15, we used a rabbit monoclonal antibody (1F7, NextCure Inc.) against the cytoplasmic domain, rigorously validated by our group previously, using the guidelines for pillars of validation[25–27]. Siglec-15 antibody validation in cell lines was done using a TMA (YTMA 403) which had both cell lines as well as tumor cores with varying expressions of Siglec-15. The cell lines included were non-transfected human embryonic kidney derived cell lines (HEK/293T) as negative controls for Siglec-15, human amelanotic melanoma cell lines (LOX-IMVI), endogenously high expressing Burkitt lymphoma cell lines (RAJI as well as RAJI transfected with Siglec-15, RAJI.S15) and primary-glioblastoma cell line (U87) cell lines which all acted as positive controls. We found the signal to noise ratio to be optimal at a concentration of 0.1 µg/ml for Siglec-15. We stained serial sections of all TMA slides for PD-L1 (clone E1L3N, optimal concentration 1.1 µg/ml) for all our experiments using a staining protocol described previously[28].

Automated quantitative analysis (AQUA) and fluorescent signal quantification

For both target proteins (Siglec-15 and PD-L1), we analyzed the fluorescent images obtained after scanning on PM-2000 platform (Navigate Biopharma, Carlsbad, CA, USA), as previously described[29]. AQUA™ method of image acquisition and protein quantification measures the target within two molecular compartments: (1) tumor, compartment generated by the cytokeratin (CK) area; and (2) stroma, a compartment created by removing the tumor compartment from the nuclear 4′,6-diamidino-2-phenylindole (DAPI) mask after appropriate dilation. QIF scores obtained represent fluorescent signal intensity divided by the compartment pixel area. Spots with inadequate tumor (<2% of the compartment area) or staining artifacts were excluded from further analyses after careful visual inspection. For each of the cohort, we stained two different blocks with cores from different areas of the tumor (twofold redundant) in independent experiments and the QIF scores presented here are the average values of the two blocks for each case.

Statistical analysis

Pearson correlation coefficient was used to analyze the linear association between two continuous variables. The *t* test or one-way analysis of variance was used to compare the means and *chi*-square test for proportions between two or more groups, respectively. For the survival analysis, tumors were split into high and low according to Siglec-15 expression using the median as a cutoff. We also searched for optimal cut-points using the the X-tiles software (https://medicine.yale.edu/lab/rimm/research/software/), but none were discovered. Survival curves were estimated using the median with the Kaplan–Meier product-limit method and the log-rank test was used for comparisons. Statistical analysis was performed using GraphPad Prism 8 software (GraphPad Software, La Jolla, CA, USA). A p value of <0.05 was considered significant.

Table 1. Overview of the cohorts of patients used in this study.

Cohort	Number (*N*)	Collection date range	Histology
YTMA 423	250	2011–2016	NSCLC
YTMA 310	120	2007–2015	NSCLC
YTMA 489	245	2011–2012	Breast
YTMA 465	70	2015–2020	HNSCC
YTMA 497	38	2015–2020	Bladder
YTMA 507	68	2015–2020	Bladder

RESULTS

Expression of Siglec-15 in different cancer types

After an extensive validation of the new Siglec-15 antibody (previously described[27], in press) we tested the validated antibody clone (1F7) on a multi-tumor tissue array (YTMA 395). Siglec-15 expression was seen both in tumor (predominantly membranous) as well as the stromal compartment (cytoplasmic expression in stromal cells). Stromal cell expression is more prevalent across all tumor types. Figure 1A, B illustrates the quantitative expression levels (represented as QIF scores) of Siglec-15 in tumor and stroma respectively across a range of different cancer types. Since this data shows high expression in NSCLC, breast, bladder and HNSCC, we focused on expression of Siglec-15 in these cancer histologies in larger cohorts towards the goal of identifying tumor types that may be good targets for anti-Siglec −15 therapy. Figure 1C, E, G, I show representative fluorescent images of high Siglec-15 expression noted in tumor while Fig. 1D, F, H, J shows high Siglec-15 in stroma for NSCLC, breast, HNSCC, and bladder cancers respectively.

Expression pattern and distribution of Siglec-15 in NSCLC

Next, we assessed the expression pattern and distribution of Siglec-15 in a larger lung cohort of 250 NSCLC cases (YTMA 423). Siglec-15 showed a wide dynamic range of expression both in tumor and stroma, depicted as continuous QIF scores (Fig. 2A, B). After careful evaluation of each spot, we defined the visual cut-point as the lowest expression with a discernable signal, above the non-specific background noise (limit of detection). Siglec-15 showed membranous or cytoplasmic staining pattern with more stromal cell expression (83% positive) than tumor cell expression (40.1%). Figure 2C, D shows representative images of Siglec-15 positivity in tumor and stromal compartments respectively. A considerable intra-tumoral heterogeneity was observed ($R^2 = 0.32$ between two blocks in tumor and $R^2 = 0.22$ between two blocks for stroma) (Fig. 2E, F). However, we noted excellent concordance for Siglec-15 between serial sections, both for tumor and stroma ($R^2 = 0.93$ in tumor and $R^2 = 0.90$ for stroma) (Fig. 2G, H). Some correlation between tumor and stromal expression was seen as well ($R^2 = 0.54$), although it was lower, partly due to lower expression in tumor compared to stroma (Fig. 2I).

Since Siglec-15 expression in NSCLC has been described to be somewhat mutually exclusive to PD-L1, we compared the expression of both proteins in our cohort in stained serial sections. The mutually exclusive pattern of expression of Siglec-15 and PD-L1 was validated in our cohort as depicted by the weak correlation between the two ($R^2 = 0.11$ in tumor and $R^2 = 0.35$ in stroma). Majority of our cases showed a lack of both the markers in tumor (54.4% negative in tumor) (Fig. 2N), while only about 6.1% were double positive (Fig. 2N). When we measured Siglec-15 and PD-L1 in the stromal compartment, we noticed a substantially higher number of cases to be positive for both the markers (48.8%), although not necessarily in the same cells. Whether this signifies co-expression by the same cells or by different population of stromal cells will be assessed in the future. Figure 2J–M shows representative images of Siglec-15 and PD-L1 in NSCLC.

Next, we proceeded to examine the prognostic significance of Siglec-15 and using median as a cutoff for the continuous QIF values, we separated our cohort into high and low expressors of Siglec-15. Siglec-15 expression in tumor did not significantly predict overall survival (OS) ($p = 0.19$) or progression-free survival (PFS) ($p = 0.24$). Similarly, neither did stromal Siglec-15 expression

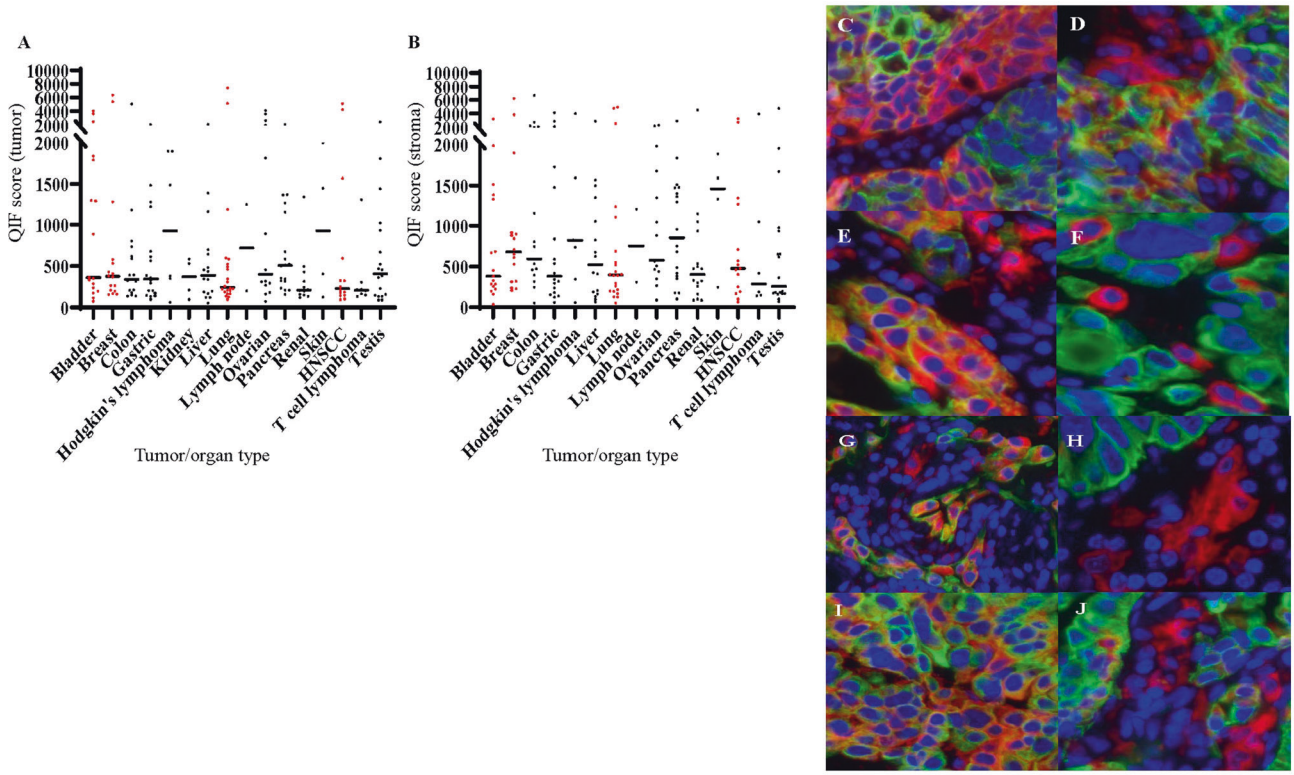

Fig. 1 Expression of Siglec-15 in different cancers by immunofluorescence (YTMA 395). **A** QIF score for Siglec-15 in the tumor compartment for the various tumor types. **B** QIF score for Siglec-15 in the stromal compartment for the various tumor types. **C–J**. Representative fluorescence images for Siglec-15 expression in tumor compartment for lung (**C**), breast (**E**), HNSCC (**G**) and bladder (**I**) and in stroma for the same (**D**), (**F**), (**H**), and (**J**).

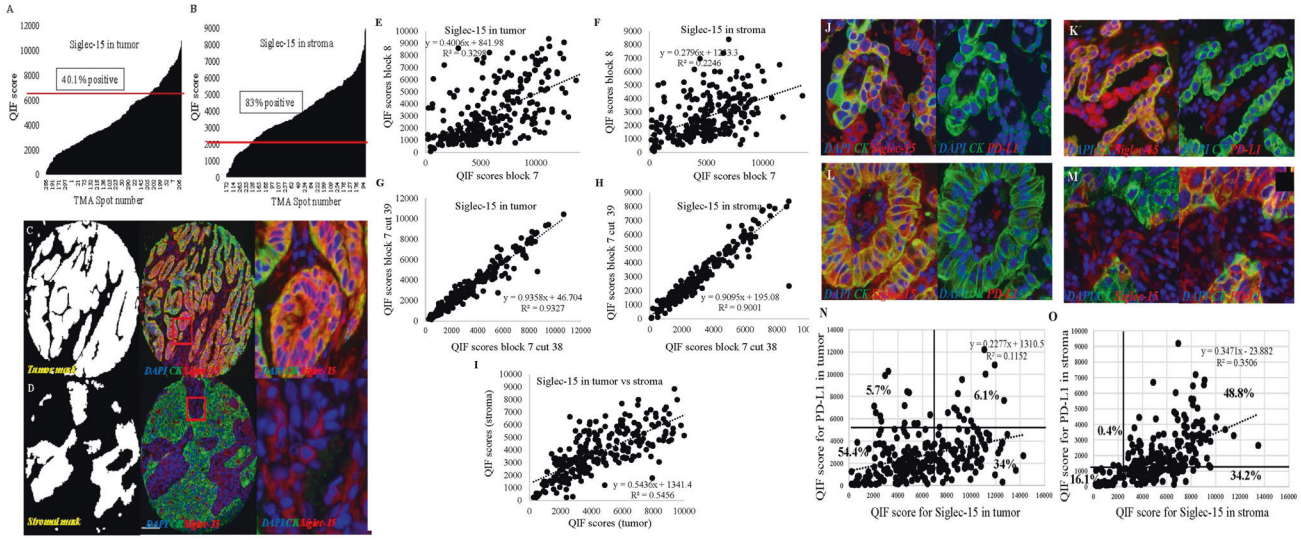

Fig. 2 Pattern of expression and distribution of Siglec-15 in NSCLC (YTMA 423). **A** Dynamic range of Siglec-15 expression in tumor. **B** Dynamic range of Siglec-15 expression in stroma. **C** Representative images of Siglec-15 tumor mask. **D** Representative images of Siglec-15 stromal mask. **E**, **F** Regressions between different blocks (tumoral heterogeneity) in tumor (**E**) and stroma (**F**). **G**, **H** Regressions between serial sections in tumor (**G**) and stroma (**H**). **I** Correlation of Siglec-15 between tumor and stroma. Association of Siglec-15 with PD-L1 expression in NSCLC. **J**–**M** Representative images of Siglec-15 expression on the left and PD-L1 on the right. **N**, **O** Correlation between Siglec-15 and PD-L1 in tumor (**N**) and stroma (**O**).

have any significant favorable prognosis for OS ($p = 0.69$) or PFS ($p = 0.94$) (see Supplementary Fig. S1).

Next, we proceeded to evaluate the association of Siglec-15 expression with the clinical characteristics and pathologic features of NSCLC. Siglec-15 in the tumor compartment was significantly lower in patients with clinical stage I ($p = 0.05$). No other significant association between tumor or stromal expression of Siglec-15 and disease stage, age, gender, histology, or smoking status was noted (Supplementary T1, T2). Neither tumor nor stromal expression of Siglec-15 demonstrated significant

associations with epidermal growth factor receptor (*EGFR*) or *KRAS* mutation status in NSCLC patients (Supplementary Fig. S6) or with tumor-infiltrating lymphocytes (TIL) (Supplementary Tables T11, T12).

Expression of Siglec-15 in breast cancer and its correlation with PD-L1

Based on our preliminary data showing high expression for Siglec-15 in a multi-tumor array, we explored expression levels in a larger breast cancer cohort (YTMA 489). Consistent with our results in NSCLC, we found a broad dynamic range of expression in both tumor and stroma, predominant in the latter. Again, employing the visual positivity cutoff, about 30.1% cases were seen to have Siglec-15 expression in tumor, while nearly double (70.1%) the cases showed stromal Siglec-15 positivity. Like in NSCLC, Siglec-15 showed a characteristic membrane or cytoplasmic localization (Fig. 3). Some intra-tumoral heterogeneity was also noticed, more in stromal expression as expected, than in tumor ($R^2 = 0.27$ between two blocks in tumor and $R^2 = 0.17$ between two blocks for stroma) (Fig. 3E, F). However, as in NSCLC, breast cancers showed excellent correlation ($R^2 = 0.82$ in tumor and $R^2 = 0.77$ for stroma) in serial sections while the tumoral and stromal Siglec-15 expression was only weakly correlated ($R^2 = 0.45$).

We further examined the association of Siglec-15 and PD-L1 in our breast cancer cohort. Compared to NSCLC, only few breast cancers showed both Siglec-15 and PD-L1 expression in the tumor compartment (0.5% in breast cancers vs. 6.1% in NSCLC) as well as stromal compartment (11% in breast cancers vs. 48.8% in NSCLC) (Fig. 3). This is consistent with generally lower levels of expression of PD-L1 in breast cancer. Survival analyses showed that Siglec-15 expression was not associated with favorable prognosis either in OS (*p value* = 0.92 in tumor and 0.89 in stroma) or in PFS (*p value* = 0.32 in tumor or 0.69 in stroma) (Supplementary S2). There was also no association between tumor or stromal S15 and stroma TIL (Supplementary Tables T13, T14).

Expression pattern and distribution of Siglec-15 in HNSCC

Next, we assessed Siglec-15 expression in a HNSCC cohort and noticed a similar pattern of expression as in NSCLC and breast cancer, with a wide dynamic range and a characteristic membranous or cytoplasmic staining in both tumor and stromal compartments. However, there was a much higher stromal positivity (95.2%) than seen in NSCLC and breast. (95.2% stromal Siglec-15 positive in HNSCC vs. 83% stromal Siglec-15 positive in NSCLC and 70.1% stromal Siglec-15 in breast) (Fig. 4). Tumor cells expressed Siglec-15 in only about 17.6% (Fig. 4A).

Some intra-tumoral heterogeneity was observed ($R^2 = 0.56$ between two blocks in tumor and $R^2 = 0.29$ between two blocks for stroma), but it was less pronounced in tumor when compared with NSCLC and breast cancer ($R^2 = 0.56$ vs. $R^2 = 0.32$ in NSCLC vs. $R^2 = 0.27$ in breast). However, we noted excellent concordance for Siglec-15 between serial sections, both for tumor and stroma ($R^2 = 0.95$ in tumor and $R^2 = 0.91$ for stroma). Tumoral and stromal expression showed a weak correlation ($R^2 = 0.25$) (Fig. 4E–I).

Serial sections stained with PD-L1 maintained the mutual exclusivity with Siglec-15 in the tumor compartment, consistent with our results for HNSCC and breast cancers. However, it was far less striking than in breast and NSCLC, as a higher number of patients showed both Siglec-15 and PD-L1 in the tumor (8.2% in HNSCC vs. 0.7% in breast vs. 6.1% in NSCLC) (Fig. 4). Siglec-15 expression, either in tumor or stroma, showed no prognostic significance as seen in the overall survival (OS) ($p = 0.54$ in tumor and $p = 0.42$ in stroma) curves (Supplementary S3).

Expression of Siglec-15 in bladder cancer

As with other cancer types in this study, Siglec-15 showed cytoplasmic and membranous localization in bladder cancers predominantly in stroma, but also in tumor (89% stromal, 5% in tumor) (Fig. 5). Serial sections showed excellent concordance both for tumor and stroma ($R^2 = 0.74$ in tumor and $R^2 = 0.65$ in stroma). Tumoral and stromal expression demonstrated a weak correlation ($R^2 = 0.55$) (Fig. 5G). Only a few bladder cancers had both Siglec-15 and PD-L1 in the stromal compartment (4%), while an even lower number had both markers in the tumor (1%), thereby validating the mutually exclusive pattern of expression between the two markers.

DISCUSSION

Previously established for its role in osteoporosis, Siglec-15 has recently been described as an important immune-regulatory target in human solid tumors by Wang et al.[24]. Its upregulation in various cancers has been documented at the mRNA level but here we examine protein expression by QIF to comprehensively characterize Siglec-15 expression with a detailed focus on lung, breast, HNSCC and bladder cancers[30–32]. Using an antibody that was rigorously validated in our previous work (Shafi et al. in press), we developed an immunofluorescence panel to detect Siglec-15

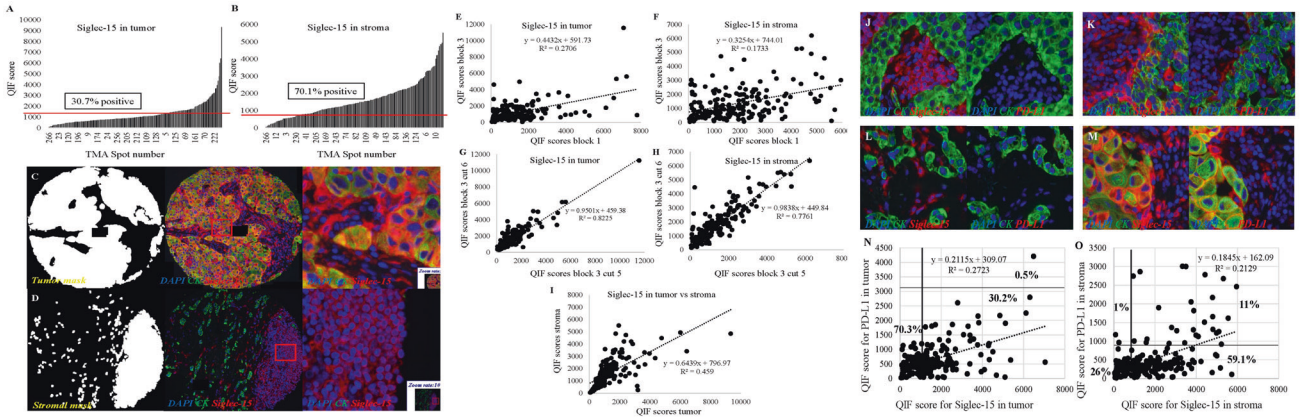

Fig. 3 Pattern of expression and distribution of Siglec-15 in breast cancer (YTMA 489). A Dynamic range of Siglec-15 expression in tumor. **B** Dynamic range of Siglec-15 expression in stroma. **C** Representative images of Siglec-15 tumor mask. **D** Representative images of Siglec-15 stromal mask. **E**, **F** Regressions between different blocks (tumoral heterogeneity) in tumor (**E**) and stroma (**F**). **G**, **H** Regressions between serial sections in tumor (**G**) and stroma (**H**). **I** Correlation of Siglec-15 between tumor and stroma. Association of Siglec-15 with PD-L1 in breast cancer. **J**–**M** Representative images of Siglec-15 expression on the left and PD-L1 on the right. **N**, **O** Correlation between Siglec-15 and PD-L1 in tumor (**N**) and stroma (**O**).

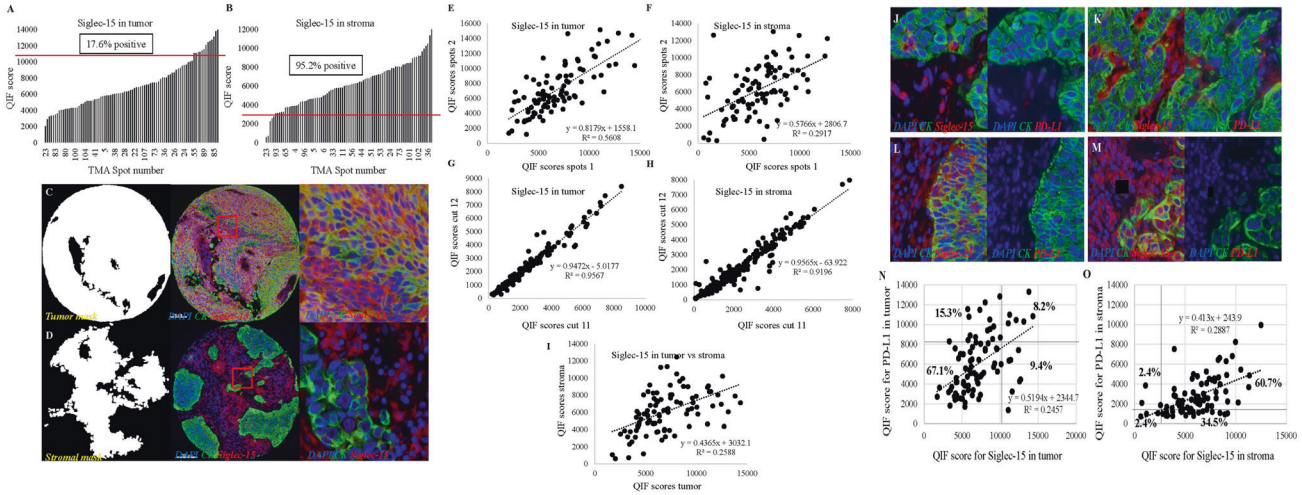

Fig. 4 Pattern of expression and distribution of Siglec-15 in HNSCC (YTMA 465). A Dynamic range of Siglec-15 expression in tumor. **B** Dynamic range of Siglec-15 expression in stroma. **C** Representative images of Siglec-15 tumor mask. **D** Representative images of Siglec-15 stromal mask. **E**, **F** Regressions between different blocks (tumoral heterogeneity) in tumor (**E**) and stroma (**F**). **G**, **H** Regressions between serial sections in tumor (**G**) and stroma (**H**). **I** Correlation of Siglec-15 between tumor and stroma. Association of Siglec-15 with PD-L1 in HNSCC. **J**–**M** Representative images of Siglec-15 expression on the left and PD-L1 on the right. **N**, **O** Correlation between Siglec-15 and PD-L1 in tumor (**N**) and stroma (**O**).

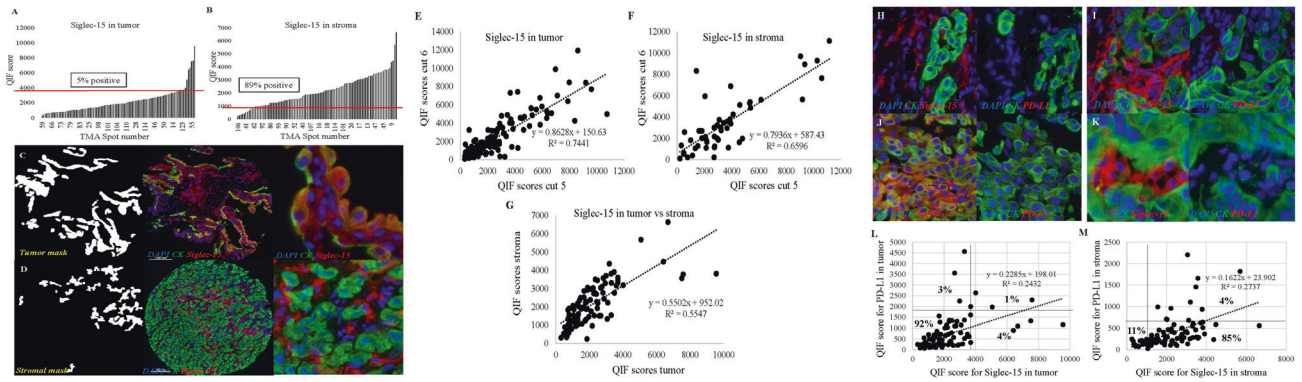

Fig. 5 Pattern of expression and distribution of Siglec-15 in bladder cancers (YTMA 507, 497). A Dynamic range of Siglec-15 expression in tumor. **B** Dynamic range of Siglec-15 expression in stroma. **C** Representative images of Siglec-15 tumor mask. **D** Representative images of Siglec-15 stromal mask. **E**, **F** Regressions between serial sections in tumor (**E**) and stroma (**F**). **G** Correlation of Siglec-15 between tumor and stroma. Association of Siglec-15 with PD-L1 in bladder cancers. **H**–**K** Representative images of Siglec-15 expression on the left and PD-L1 on the right. **L**, **M** Correlation between Siglec-15 and PD-L1 in tumor (**L**) and stroma (**M**).

and quantify protein levels with molecular compartments. We found Siglec-15 to be expressed both in the tumor (defined by co-localization with cytokeratin) and stroma (not co-localized with cytokeratin), with stromal expression being predominant across various cancer types. Siglec-15 exhibited a heterogenous pattern of expression, with some areas demonstrating high expression and others low, or even negative within the same tumor. Tumoral Siglec-15 staining was consistent among different cores of the same tumor, with stromal staining less so. Significantly high Siglec-15 expression in tumor was seen in poorly differentiated invasive ductal breast cancers. No association is found between Siglec-15 expression and clinicopathologic characteristics or outcome.

In their study, Wang et al. highlighted the somewhat mutually exclusive pattern of expression of Siglec-15 and PD-L1 and they found co-expression of both the markers in a very small number of the 218 NSCLC patients they examined (3.2%)[24]. While our study validated this mutual exclusivity of Siglec-15 and PD-L1 in breast, bladder and HNSCC in addition to previously described NSCLC, we identified a higher percentage of patients expressing both Siglec-15 and PD-L1 across all cancer types studied (6.1% in tumor and 48.8% in stroma in NSCLC, 0.5% in tumor and 11% in stroma in breast cancers, 8.2% in tumor and 60.2% in stroma in HNSCC and 1% in tumor and 4% in stroma in bladder cancers). This could be due to a much higher affinity, novel antibody used in this study. Previously we used a commercially available polyclonal antibody since for this discovery work monoclonals were not yet available. As seen previously, we also found Siglec-15 expression both in tumor and stromal immune cells in all the four cancer types. In contrast to the initial data in NSCLC, we found Siglec-15 to be more abundantly expressed by stromal immune cells rather than by tumor cells (22.8% in tumor and 13.3% in stroma vs. 40.1% in tumor and 83% in stroma in our study) in our lung cancer cohort[24]. The higher percentage of both tumor and stromal positivity in our study of NSCLC could be due to higher affinity of our rabbit monoclonal antibody clone and the optimized assay. It is notable that the mutual exclusivity noted is predominantly in tumor staining. The stromal or immune cell staining shows more co-expression of both PD-L1 and S15. This may suggest different mechanism of expression in the tumor cells compared to immune cells. Note also that since S15 and PD-L1 were not multiplexed, it could be that different stromal immune cells are expressing the respective proteins.

Another important finding in our study has been the demonstration of new potential candidates for anti-Siglec-15 immunotherapy, other than NSCLC. We found elevated Siglec-15 expression in lung, breast, bladder, HNSCC, colon, liver, pancreatic and renal cancers in our study. This is in agreement with the results published by Wang et al. that showed upregulation of Siglec-15 at the mRNA level using TCGA data in bladder, colon, endometrioid, renal, liver and thyroid cancers[24]. Currently, a Phase II trial to test the effect of a humanized mAb to Siglec-15 in NSCLC (NC318) is ongoing. While it is too early to assess response, our results show that besides NSCLC, breast, HNSCC and bladder cancers may be other suitable candidates for anti-Siglec-15 therapy.

Our study has several limitations. First, this broad screening study was done entirely on tissue microarrays. While TMAs are a useful tool, further validation with whole tissue sections is required for final assay development of clinical evaluation of patients. Secondly, our NSCLC cohort is comprised mostly of early-stage patients with surgically resectable disease, thus future studies are required for the evaluation of distribution and prognostic significance of this marker in advanced-stage NSCLC. Finally, this work was done on retrospective collection of tissue without standardization of treatment. While Siglec 15 was not associated with outcome in any organ system assessed here, we recognize the limitations of retrospective, variable treatment, cohorts.

To conclude, we show the landscape of expression of Siglec-15 in lung, breast, head and neck and bladder cancers as well as highlight its association with PD-L1 by QIF using a validated, high-affinity monoclonal antibody. This work lays the groundwork for design of future single agent or combinatorial clinical trials with Siglec-15 inhibitors in a range of epithelial cancers.

REFERENCES

1. Gandhi, L., Rodriguez-Abreu, D., Gadgeel, S., Esteban, E., Felip, E., De Angelis, F. *et al*. Pembrolizumab plus Chemotherapy in Metastatic Non-Small-Cell Lung Cancer. *N Engl J Med* 378, 2078-2092 (2018).
2. Garon, E. B., Hellmann, M. D., Rizvi, N. A., Carcereny, E., Leighl, N. B., Ahn, M.-J. *et al*. Five-year overall survival for patients with advanced non–small-cell lung cancer treated with pembrolizumab: results from the phase I KEYNOTE-001 study. *J Clin Oncol* 37, 2518 (2019).
3. Schmid, P., Cortes, J., Pusztai, L., McArthur, H., Kummel, S., Bergh, J. *et al*. Pembrolizumab for Early Triple-Negative Breast Cancer. *N Engl J Med* 382, 810-821 (2020).
4. Voorwerk, L., Slagter, M., Horlings, H. M., Sikorska, K., van de Vijver, K. K., de Maaker, M. *et al*. Immune induction strategies in metastatic triple-negative breast cancer to enhance the sensitivity to PD-1 blockade: the TONIC trial. *Nat Med* 25, 920-928 (2019).
5. Dirix, L. Y., Takacs, I., Jerusalem, G., Nikolinakos, P., Arkenau, H.-T., Forero-Torres, A. *et al*. Avelumab, an anti-PD-L1 antibody, in patients with locally advanced or metastatic breast cancer: a phase 1b JAVELIN Solid Tumor study. *Breast Ca Res Treat* 167, 671-686 (2018).
6. Adams, S., Schmid, P., Rugo, H., Winer, E., Loirat, D., Awada, A. *et al*. Pembrolizumab monotherapy for previously treated metastatic triple-negative breast cancer: cohort A of the phase II KEYNOTE-086 study. *Annals Oncol* 30, 397-404 (2019).
7. Emens, L. A., Cruz, C., Eder, J. P., Braiteh, F., Chung, C., Tolaney, S. M. *et al*. Long-term clinical outcomes and biomarker analyses of atezolizumab therapy for patients with metastatic triple-negative breast cancer: a phase 1 study. *JAMA Oncol* 5, 74-82 (2019).
8. Nanda, R., Chow, L. Q., Dees, E. C., Berger, R., Gupta, S., Geva, R. *et al*. Pembrolizumab in patients with advanced triple-negative breast cancer: phase Ib KEYNOTE-012 study. *J Clin Oncol* 34, 2460 (2016).
9. Schmid, P., Adams, S., Rugo, H. S., Schneeweiss, A., Barrios, C. H., Iwata, H. *et al*. Atezolizumab and nab-paclitaxel in advanced triple-negative breast cancer. *New Eng J Med* 379, 2108-2121 (2018).
10. Lyford-Pike, S., Peng, S., Young, G. D., Taube, J. M., Westra, W. H., Akpeng, B. *et al*. Evidence for a role of the PD-1:PD-L1 pathway in immune resistance of HPV-associated head and neck squamous cell carcinoma. *Cancer Res* 73, 1733-1741 (2013).
11. Kok, V. C. Current Understanding of the Mechanisms Underlying Immune Evasion From PD-1/PD-L1 Immune Checkpoint Blockade in Head and Neck Cancer. *Front Oncol* 10, 268 (2020).
12. Burtness, B., Harrington, K. J., Greil, R., Soulieres, D., Tahara, M., de Castro, G., Jr *et al*. Pembrolizumab alone or with chemotherapy versus cetuximab with chemotherapy for recurrent or metastatic squamous cell carcinoma of the head and neck (KEYNOTE-048): a randomised, open-label, phase 3 study. *Lancet* 394, 1915-1928 (2019).
13. Qiao, X. W., Jiang, J., Pang, X., Huang, M. C., Tang, Y. J., Liang, X. H. *et al*. The Evolving Landscape of PD-1/PD-L1 Pathway in Head and Neck Cancer. *Front Immunol* 11, 1721 (2020).
14. Bauml, J., Seiwert, T. Y., Pfister, D. G., Worden, F., Liu, S. V., Gilbert, J. *et al*. Pembrolizumab for platinum-and cetuximab-refractory head and neck cancer: results from a single-arm, phase II study. *J Clin Oncol* 35, 1542 (2017).
15. Cohen, E. E., Soulières, D., Le Tourneau, C., Dinis, J., Licitra, L., Ahn, M.-J. *et al*. Pembrolizumab versus methotrexate, docetaxel, or cetuximab for recurrent or metastatic head-and-neck squamous cell carcinoma (KEYNOTE-040): a randomised, open-label, phase 3 study. *Lancet* 393, 156-167 (2019).
16. Powles, T., Csoszi, T., Ozguroglu, M., Matsubara, N., Geczi, L., Cheng, S. Y. *et al*. Pembrolizumab alone or combined with chemotherapy versus chemotherapy as first-line therapy for advanced urothelial carcinoma (KEYNOTE-361): a randomised, open-label, phase 3 trial. *Lancet Oncol* 22, 931-945 (2021).
17. Stenehjem, D. D., Tran, D., Nkrumah, M. A. & Gupta, S. PD1/PDL1 inhibitors for the treatment of advanced urothelial bladder cancer. *Onco Targets Ther* 11, 5973-5989 (2018).
18. Powles, T., Durán, I., Van Der Heijden, M. S., Loriot, Y., Vogelzang, N. J., De Giorgi, U. *et al*. Atezolizumab versus chemotherapy in patients with platinum-treated locally advanced or metastatic urothelial carcinoma (IMvigor211): a multicentre, open-label, phase 3 randomised controlled trial. *Lancet* 391, 748-757 (2018).
19. Powles, T., van der Heijden, M. S., Castellano, D., Galsky, M. D., Loriot, Y., Petrylak, D. P. *et al*. Durvalumab alone and durvalumab plus tremelimumab versus chemotherapy in previously untreated patients with unresectable, locally advanced or metastatic urothelial carcinoma (DANUBE): a randomised, open-label, multicentre, phase 3 trial. *Lancet Oncol* 21, 1574-1588 (2020).
20. Vuky, J., Balar, A. V., Castellano, D., O'Donnell, P. H., Grivas, P., Bellmunt, J. *et al*. Long-term outcomes in KEYNOTE-052: phase II study investigating first-line pembrolizumab in cisplatin-ineligible patients with locally advanced or metastatic urothelial cancer. *J Clin Oncol* 38, 2658-2666 (2020).
21. Adams, O. J., Stanczak, M. A., von Gunten, S. & Laubli, H. Targeting sialic acid-Siglec interactions to reverse immune suppression in cancer. *Glycobiology* 28, 640-647 (2018).
22. Crocker, P. R. & Varki, A. Siglecs, sialic acids and innate immunity. *Trends Immunol* 22, 337-342 (2001).
23. Varki, A. & Angata, T. Siglecs--the major subfamily of I-type lectins. *Glycobiology* 16, 1R-27R (2006).
24. Wang, J., Sun, J., Liu, L. N., Flies, D. B., Nie, X., Toki, M. *et al*. Siglec-15 as an immune suppressor and potential target for normalization cancer immunotherapy. *Nat Med* 25, 656-666 (2019).
25. Uhlen, M., Bandrowski, A., Carr, S., Edwards, A., Ellenberg, J., Lundberg, E. *et al*. A proposal for validation of antibodies. *Nat Methods* 13, 823-827 (2016).
26. MacNeil, T., Vathiotis, I. A., Martinez-Morilla, S., Yaghoobi, V., Zugazagoitia, J., Liu, Y. *et al*. Antibody validation for protein expression on tissue slides: a protocol for immunohistochemistry. *Biotechniques* 69, 460-468 (2020).
27. Shafi, S., Aung, T. N., Robbins, C., Zugazagoitia, J., Vathiotis, I. A., N. Gavrielatou *et al*. Development of an Immunohistochemical Assay for Siglec-15 *Lab Invest* (2022).
28. Velcheti, V., Schalper, K. A., Carvajal, D. E., Anagnostou, V. K., Syrigos, K. N., Sznol, M. *et al*. Programmed death ligand-1 expression in non-small cell lung cancer. *Lab Invest* 94, 107-116 (2014).
29. Camp, R. L., Chung, G. G. & Rimm, D. L. Automated subcellular localization and quantification of protein expression in tissue microarrays. *Nat Med* 8, 1323-1327 (2002).
30. Li, B., Zhang, B., Wang, X., Zeng, Z., Huang, Z., Zhang, L. *et al*. Expression signature, prognosis value, and immune characteristics of Siglec-15 identified by pan-cancer analysis. *Oncoimmunology* 9, 1807291 (2020).
31. Li, Q. T., Huang, Z. Z., Chen, Y. B., Yao, H. Y., Ke, Z. H., He, X. X. *et al*. Integrative Analysis of Siglec-15 mRNA in Human Cancers Based on Data Mining. *J Cancer* 11, 2453-2464 (2020).
32. Hu, J., Yu, A., Othmane, B., Qiu, D., Li, H., Li, C. *et al*. Siglec15 shapes a non-inflamed tumor microenvironment and predicts the molecular subtype in bladder cancer. *Theranostics* 11, 3089-3108 (2021).

ACKNOWLEDGEMENTS

We would like to thank Lori Charette, Deirdre H. Salemme, Amos Brooks, Patricia Gaule, and the team at the Yale Pathology Tissue Service and Developmental Histology Facility for production of the high-quality tissue sections.

AUTHOR CONTRIBUTIONS

S.S.: Formal analysis, investigation, visualization, methodology, writing–original draft, writing–review, and editing. T.N.A.: Data curation, formal analysis, validation, visualization, methodology, writing (review and editing). V.X.: Data validation, visualization. N.G.: Investigation, visualization, methodology, writing (review and editing). I.V.: Data curation, formal analysis, validation, visualization, methodology, writing (review and editing). A.F.: Investigation, visualization, methodology, writing (review and editing). M.M.: Investigation, visualization, methodology, writing (review and editing). V.Y.: Investigation, visualization, methodology, writing (review and editing). R.S.H.: Resources, project administration, writing (review and editing). L.N.L.: Resources, project administration, writing (review and editing). S.L.: Resources, project administration, writing (review and editing). D.L.R.: Conceptualization, resources, formal analysis, supervision, funding acquisition, writing–original draft, project administration, writing–review, and editing.

FUNDING

This work is supported by sponsored research agreement from NextCure Inc. D.L.R. and R.S.H. are also supported by the Yale SPORE in Lung Cancer (P50CA196530) and the Yale Cancer Center CCSG (P30CA016359).

COMPETING INTERESTS

D.L.R. has served as an advisor for Astra Zeneca, Agendia, Amgen, BMS, Cell Signaling Technology, Cepheid, Daiichi Sankyo, Novartis, GSK, Konica Minolta, Merck, NanoString, PAIGE.AI, Perkin Elmer, Roche, Sanofi, Ventana and Ultivue. Amgen, Cepheid, Konica Minolta, NavigateBP, NextCure, and Lilly fund research in his lab. L.N.L., and S.L. are employees of NextCure. J. Zugazagoitia has served as an advisor for BMS, Novartis, Guardant Health and he reports speaker's honoraria from BMS, Pfizer, Roche, Astra Zeneca, and Guardant Health. Astra Zeneca funds research in his lab. All other authors declare no competing interests.

ETHICS APPROVAL AND CONSENT TO PARTICIPATE

All tissue samples were collected with the approval from the Yale Human Investigation Committee protocol #9505008219. Written informed consent, or waiver of consent, was obtained from all patients with the approval of the Yale Human Investigation Committee in accordance with the Declaration of Helsinki.

ADDITIONAL INFORMATION

Supplementary information The online version contains supplementary material available at https://doi.org/10.1038/s41374-022-00796-6.

Correspondence and requests for materials should be addressed to David L. Rimm.

Reprints and permission information is available at http://www.nature.com/reprints

Publisher's note Springer Nature remains neutral with regard to jurisdictional claims in published maps and institutional affiliations.